Limitations Imposed by Beam-Beam Effects and Their Remedies II

J. E. Spencer

Stanford Linear Accelerator Center, Stanford University, Stanford, CA 94309

Invited Talk **e-e-** 1999: Electron-Electron Interactions at TeV Energies
Santa Cruz, CA, December 10-12, 1999

LIMITATIONS IMPOSED BY BEAM-BEAM EFFECTS AND THEIR REMEDIES - II

J.E. SPENCER[*]

Stanford Linear Accelerator Center
Stanford University, Stanford, CA 94309, USA

Effects that limit the luminosities of a general purpose linear collider (GLC) capable of $\vec{e}^{\pm}\vec{e}^{\pm}$, $\vec{\gamma}\vec{e}^{\pm}$ and $\vec{\gamma}\vec{\gamma}$ channels are discussed together with mitigations. Previous results are extended to understand the differences between channels to maximize the generalized luminosity. A standard NLC configuration at $\sqrt{s}_{ee}$= 0.5 TeV is used for comparison. Without charge compensation or bunch shaping, such flat beam configurations (aspect ratios $R^{*} \gg 1$) imply major disadvantages for $e^{-}e^{-}$ due to the strong disruption (D) and small, longitudinal f-numbers($f_l \# \equiv \beta_y^{*}/\sigma_z$) that are imposed. Previous round and flat beam configurations are studied as functions of D(or $f_b\#$), $f_l\#$ and the constraints Δ_B, N_γ and Υ. Round beams with decreased disruptions and larger f_l-stops are preferred with tensor beams, charge compensation or other bunch manipulation schemes. A low energy, high luminosity prototype is again proposed based on the possible physics.

1. Introduction

In the first $e^{-}e^{-}$ workshop[1,2] we looked at $\vec{e}^{-}\vec{e}^{-}$ because electrons would be used to produce the other channels and because $e\gamma$ and $e^{-}e^{-}$ collisions could provide new physics at SLC energies[3] given an improved configuration or one compatible with such channels that provided an increased geometric luminosity $\mathcal{L}_{G}(e^{+}e^{-})$. Further, because the beam dynamics of the $e^{+}e^{-}$ channel had been verified reasonably well at the SLC and studied further for the NLC[4] at higher energies, work concentrated on determining the achievable luminosities in these other channels in a way that was consistent with a standard NLC $e^{+}e^{-}$ configuration. A generalized luminosity[2,5] was then defined, calculated and discussed at these workshops. While the production of e^{+} and especially $\vec{e}^{+}$ was an important distinguishing complication for $e^{+}e^{-}$, the more evident difference with $e^{-}e^{-}$ resulted from beam-beam disruption effects. A typical result, first presented in Ref. 2, was a factor of three or so in luminosity.

This ratio can never approach one for the present NLC configuration regardless of the disruption without 'shorter' bunches. The solution to this problem is also a requirement for higher frequency acceleration. For very high frequencies, tensor beams[5] with low, single-bunch charges are required. Analytic calculations for the beam-beam effects are then possible that simplify optimization. Based on the next generation linac, the incremental costs incurred for a GLC should be modest and should also provide advantages for $e^{+}e^{-}$. Finally, we revisit the physics potential of a GLC at SLC energies when much higher luminosities are possible.

2. Previous Results, Parameters and Scalings

The most important technical figure-of-merit for colliders is the total, integrated, usable luminosity. The generalized luminosity[2,5] is based on the observation that **all** colliding beam machines as well as **all** incident channels in any particular GLC can be expected to have a luminosity that is proportional to the square of the incident bunch charges (fN_e^2 or $n_B fN_e^2$ or $n_x n_y n_z fN_e^2$) that can be brought into collision per unit time within an effective area that is minimal subject to various conversion and detector constraints.

2.1. *The Generalized Luminosity $\mathcal{L}$*

For gaussian incident bunches, the standard expression for the luminosity $\mathcal{L}$, in terms of the particles in a single bunch N_B and the undisrupted, rms spot sizes $\sigma_{x,y}^*$ at the interaction point[a] is:

$$\mathcal{L} = \frac{f_T n_B N_B^2 H_D}{4\pi\sigma_x^*\sigma_y^*}\zeta \equiv \mathcal{L}_{\mathrm{G}} H_D \zeta \rightarrow \frac{f_T n_B N_B^2 \gamma H_D}{4\pi\epsilon_n\beta^*}\,\zeta = \frac{f_T n_B N_B^2 \gamma}{4\pi\widehat{\sigma}^2}\,\zeta \propto \frac{P_b}{\widehat{\sigma}^2}\Big(\frac{\widehat{N}_B^2}{N_B}\Big)\zeta'$$

where n_B is the number of bunches in a train and f_T is the RF rep-rate (the number of bunch trains/s). The arrow implies round beams. The dimensionless parameter H_D is the luminosity 'enhancement' defined in terms of the geometric luminosity as $\mathcal{L}/\mathcal{L}_{\mathrm{G}}$ when the efficiency factor $\zeta=1$. $\zeta'\gg1$ is possible and this may change H_D. The electron beam power $P_b \propto fnN$ while ϵ_n is the invariant emittance and β^* is the magneto-optical 'depth of field' at the IP equivalent to the Rayleigh range Z_R for lasers. β^* is related to the bunch length $\sigma_z^*(=\sigma_z)$ at the IP such that 'short' bunches will be said to have large, longitudinal f_l-stops defined by $f_l\#\equiv\beta_y^*/\sigma_{\mathrm{z}}$. One can show that $\beta^*\approx f^*\delta_{stop}$ with δ_{stop} the largest energy spread that allows $\delta\sigma_y^*/\sigma_y^* \leq 1$.

For a 'tensor' accelerator, we add two transverse variables (n_x, n_y) that count the number of 'accelerators' or beams in the transverse plane. $n_q(=1$ or $2)$ will give the number of charge species in N_B and the number of bunches in any one train becomes $n_z=n_B$. One example, that takes advantage of silicon, integrated circuit technology, illustrated[5] some charge compensation schemes that could curtail beamsstrahlung. The generalized luminosity becomes:

$$\mathcal{L} = \frac{n_x n_y n_z}{n_q}\frac{f_T (N_B n_q)^2 H_D}{4\pi\sigma_x^*\sigma_y^*}\zeta = n_x n_y n_z n_q \frac{f_T \widehat{N}_B^2}{4\pi\widehat{\sigma}_x\widehat{\sigma}_y}\zeta'\;.$$

This is a good example of why we specifically avoided labels on the luminosity or the number of electrons in a bunch N_B. If we take $n_x=2n_y=2$ and accelerate equal bunches of e^+ and e^-, as illustrated previously (Fig. 5 in Ref. 5), we expect

$$\mathcal{L}(n_x=2,n_y=1,n_z=1,\; n_q=2) = 4\mathcal{L}(n_x=n_y=n_z=n_q=1) = \mathcal{L}(e^-e^-)+2\mathcal{L}(e^+e^-)+\mathcal{L}(e^+e^+)$$

assuming perfect alignment and charge compensation. Clearly, higher luminosities are possible in any number of conceivable configurations. With less than one event per crossing, this should be a viable operating configuration capable of new physics.

---

[a]These are understood to be the predicted rms sizes from high order magneto-optical simulations.[6]

2.2. *The Disruption Parameter D (or Longitudinal Beam-Beam Stop)*

The beam-beam interaction couples the particle detector to the accelerator and constrains the machine luminosity through the backgrounds and occupancy rates. Assuming unperturbed gaussian bunches at the IP, the linearized, equivalent, beam-beam focal length[7] is:

$$\frac{1}{f_{b_{x,y}}} = \pm\frac{2N_B r_e}{\gamma\sigma_{x,y}(\sigma_x + \sigma_y)} \equiv \frac{D_{x,y}}{\sigma_z} \equiv \frac{\theta_D}{\sigma_{x,y}} \ .$$

θ_D is a characteristic angle for the full-energy, primary, disrupted particles. $\sigma_{x,y}/\sigma_z$ is called the diagonal angle θ_d and equals θ_D when $D_{x,y}=1$. The $\pm$ sign implies focusing(+) for e^+e^- and defocusing(-) for e^-e^-.

Although D enhances luminosity in the e^+e^- channel, D and θ_D are related to the beam-beam strength parameter (tune shift or more properly the 'spread') in storage rings[8] ($\xi=\beta^*/4\pi f_b$) that characterizes their luminosity limits. Having defined a longitudinal f-stop for the external beam optics as $f_l\# \equiv \beta_y^*/\sigma_z$, we will call the inverse of D, the longitudinal f-stop due to beam-beam focusing $f_b\#$. Matching these gives

$$\frac{f_b}{\sigma_z} = \frac{1}{D} = \frac{\beta_y^*}{\sigma_z} \geq 1 \implies D \leq 1 \ .$$

As for conventional optics, the larger the f-stop the simpler and less expensive the optics. Also, this regime greatly simplifies multibunch beam-beam calculations.

In the e^+e^- channel, the maximum disruption angle is in the horizontal with $\theta_{x,max}=\theta_D$ because the disruption D_y is so large that it produces over focusing or a thick lens effect whereas the focusing over the length of the beam in x is weaker but cumulative or more like a thin lens[2]. For e^-e^- the situation reverses and the vertical disruption angle dominates. In either case, θ_D is typically an order of magnitude larger than for the rms divergence angles of the incident beams at the IP for all current configurations.

Because $D_{x,y}$ varies with energy, the effective D varies greatly between incident channels and the detector field seriously influences the outgoing beams. Thus, while large values of D enhance the geometric luminosity for e^+e^-, they provide serious challenges for the extraction line[9] and for e^-e^- as well as for the constraints discussed in the next section. Although the strong, nonlinear, nonconservative nature of the beam-beam interaction is extremely interesting, representative calculations show that large D's are not necessary even for e^+e^-.

2.3. *The Physics and Detector Constraint Parameters Υ, N_γ and Δ_B*

Υ is a QED invariant measure of the beam induced field strength that drives the beam-beam interaction[2] and produces beamsstrahlung and pairs. Using the expression for the average, unperturbed, gaussian bunch[10] with small D,

$$\Upsilon_{\text{eff}} \ = \ \frac{\gamma}{\text{B}_{\text{crit}}}\text{B}_{\text{eff}} = \frac{\gamma r_e^2}{\alpha e}\text{B}_{\text{eff}} = \frac{5}{6}\left[\frac{\gamma r_e^2}{\alpha\sigma_z}\right]\frac{N_B}{\widehat{\sigma}_x + \widehat{\sigma}_y}$$

where $\widehat{\sigma}$ is understood to be the perturbed, effective beam size from disruption and optics so that $\widehat{\sigma} = \sigma^*/H^{1/2}$ for round beams from the expression for $\mathcal{L}$ given above.

Similarly, the number of photons per electron, N_γ, and the rms energy loss[11] due to beamsstrahlung, δ_B, are proportional to some power of Υ or preferably Υ_{eff} when calculable. Although $\Upsilon \leq 0.3$ is a typical limit to control beamsstrahlung and pair backgrounds there is no consensus because it depends on the beam aspect ratio R. One reason why people concentrate on flat beams follows from D, Υ and N_γ together with the desire to enhance $\mathcal{L}$ using disruption. However, even without disruption, small f_l-stops produce an hourglass effect that favors flat beams.

The mean number of photons produced per electron per bunch crossing, N_γ, based on using an unperturbed expression[12] with similar assumptions as above, is

$$N_\gamma \;\approx\; \frac{5}{2}\left[\frac{\alpha\sigma_z}{\gamma\lambda_{\text{C}}}\right]\frac{\Upsilon_{\text{eff}}}{\left(1 + \Upsilon_{\text{eff}}^{\,2/3}\right)^{1/2}} \;.$$

This agrees well with PIC simulations. Using it, one can approximate the fraction of electrons per bunch that survive with full energy. We called this $\mathcal{L}_{100}/\mathcal{L}_{e\pm}$ in Ref's. 2 and 5 where we calculated it with a modified version of the PIC simulation code ABEL[13] that included $e^- e^-$

$$\mathcal{L}_{100}/\mathcal{L} \;\approx\; \frac{1}{N_\gamma^{\,2}}\left(1 - \exp\left(-N_\gamma\right)\right)^2 \;.$$

Finally, $\langle E_i - E_o\rangle/E_i$, the normalized, average beamsstrahlung energy loss per electron per bunch crossing, based on the previous assumptions, is

$$\Delta_B \equiv \frac{\langle E_i - E_o\rangle}{E_i} \;\approx\; \frac{1}{2}N_\gamma\,\Upsilon_{\text{eff}}\frac{\left(1 + \Upsilon_{\text{eff}}^{\,2/3}\right)^{1/2}}{\left(1 + (1.5\Upsilon_{\text{eff}})^{2/3}\right)^2} \;.$$

If we write Δ_B in a more familiar form and compare it to the luminosity expression for round beams, we see that it varies in the same way as $\gamma N^2/\widehat{\sigma}^2$ – ignoring a quantum efficiency factor that varies rather slowly between $0 \to 1$. Normalizing the luminosity to $\mathcal{L}_\Delta \propto \mathcal{L}/\Delta_B$ so that $\mathcal{L}_\Delta(\text{Round}) = 1$ gives

$$\frac{\mathcal{L}_\Delta(\text{Flat})}{\mathcal{L}_\Delta(\text{Round})} = \frac{(1 + \text{R})^2}{4R} \;.$$

This clearly indicates a preference for flat beams with $\text{R} \gg 1$, apart from concerns such as collisional stability, because it increases the usable machine luminosity.

The expressions above have been checked with ABEL simulations and the ABEL simulations were spot-checked with Guinea Pig[14] – also available at SLAC. As one can verify from the Tables in Ref's. 2 and 5, they are quite adequate with the possible exception of Δ_B for large D. This is especially true for the low D regime of interest here where single-bunch, single-electron multiphoton processes should be rare. Thus, all we need is to calculate the enhancement factor H_D or $\mathcal{L}$.

2.4. Analytic Approximations for $\mathcal{L}$

While there is no self-consistent theory of beam-beam effects, approximations lead to analytic expressions for $\mathcal{L}$ and therefore the physics and detector constraints.

For example, with gaussian bunches and no disruption, the normalized luminosity $\mathcal{L}_N \equiv \mathcal{L}/\mathcal{L}_G$ is a function of only one system parameter, the $f_l\#$ or simply f_l here:

$$\mathcal{L}_N(\text{Round}) \propto \text{F}(f_l)\ \text{Erfc}(f_l{}^2)$$

and

$$\mathcal{L}_N(\text{Flat}) \propto \text{F}(f_l)\text{K}_0(f_l{}^2) > \mathcal{L}_N(\text{Round})$$

where K_0 is a modified Bessel function. The ratio of these expressions, for $0 < f_l \ll 1$, grows logarithmically, favoring flat beams, small f_l and f_b stops (large disruptions). For $f_l\#$, $f_b\#{\geq}1$ ($D{\leq}1$), a constraint on $\mathcal{L}_{\text{GLC}}$ for a tensor accelerator, one finds

$$\mathcal{L}_N(\text{Flat})/\mathcal{L}_N(\text{Round}) \leq \frac{0.85}{0.76} = 1.12\ .$$

From the foregoing, it is clear that the essential parameters that characterize the problem, apart from important practical considerations, are $f_l\#$, $f_b\#$, Υ_{eff} and R. This assumes, of course, that we have determined $\mathcal{L}$ or the disruption factor H_D adequately.

2.5. *Recent Results and Comparisons*

Fig. 1 shows predictions for the standard e^+e^- NLC design[4,2] at $\sqrt{s}_{\text{ee}}= 0.5$ TeV whose layout[4,5] was the basis for all of the calculations discussed in Ref. 4. We have made calculations for this configuration for both e^+e^- and e^-e^- as a function of D_y because this defines the practically achievable e^- beams for the NLC and therefore a realistic value for $\mathcal{L}(e^-e^-)$. The results of that assumption, for these two channels, were summarized in Table I of Ref. 2 and Table II of Ref. 5 for one value of D_y, shown in Fig. 1, that yielded acceptable constraint parameters for e^+e^-. The corresponding value for the e^-e^- channel, based on the same value of Υ_{eff}, is slightly off scale in Fig. 1.
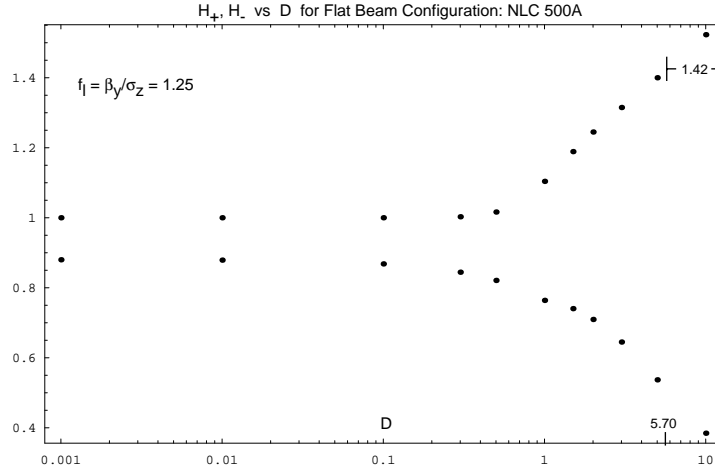

Fig. 1. $e^-e^\pm$ predictions for the standard e^+e^- NLC design[4,2,5] at $\sqrt{s}_{\text{ee}}= 0.5$ TeV.

It is important to note that we have shown H_+ relative to its undisrupted analytic representation to show that the effects of the two f-stops don't factorize, i.e., $H_D \neq H_{f_b} H_{f_l}$. This is the only case where we do this so that H_- converges to 0.88. In Fig. 2, where $f_l\#=5$, the asymptotic values approach 1 to within a few percent. This provides a good example of the 'weak focusing' regime that we will describe loosely as $f_l\#, f_b\# \geq 5$ ($D \leq 0.2$).
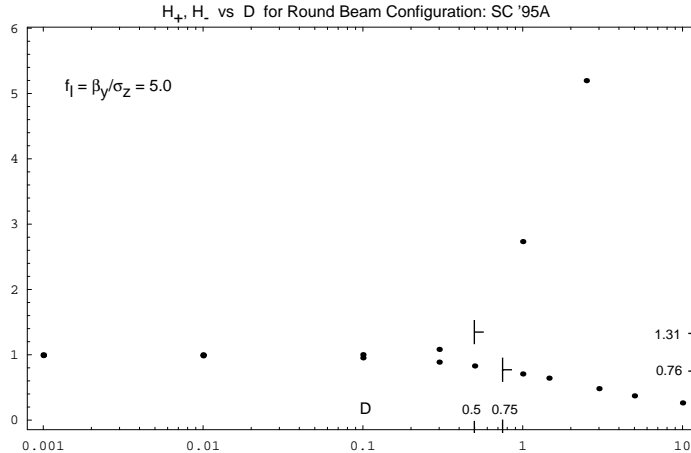
Fig. 2. $e^- e^\pm$ predictions for a round beam configuration[2] at $\sqrt{s}_{ee} = 0.5$ TeV.

Round beam configuration SC'95A in Fig. 2 was studied[2] in the first Workshop. It allowed 1 nC bunches without using damping rings – a serious imposition for tensor beams. It demonstrates previous analytic conclusions, e.g., lower disruptions are necessary for acceptable values of Υ_{eff} but this makes the $e^+ e^-$ and $e^- e^-$ channels compatible. For flat beams, $\mathcal{L}_+/\mathcal{L}_- = 2.6$ (1.7 for round) but $\mathcal{L}(e^+ e^-)$ is reduced.

3. New Acceleration Techniques and Bunch Combination Schemes

While several approaches are being pursued, one that appears well suited to solve a number of problems for a GLC is vacuum laser acceleration discussed[5] in the last workshop. Fig. 3 shows a practical example for an accelerator cell that is being studied by Tomas Plettner of the LEAP[15] collaboration. In this planar view, a single, linearly-polarized laser beam is split and the two halves are crossed in the cell to provide a longitudinal accelerating field. The light enters on one side and exits on the other at the Brewster angle in such a way that it can then be reused to improve efficiency.

Because one intends to fabricate these structures using integrated circuit techniques, one can as easily make an array or matrix of these on a single wafer. Light from high-power, diode-pumped lasers can be split into several parts (e.g. n_z) for multicell, tensor acceleration as shown in Fig. 5 of Ref. 5. In that example, we illustrated charge compensation with $n_x=2$, $n_y=1$ and $n_q=2$ using equal bunches of e^+ and e^- to give $\mathcal{L} \approx 4\mathcal{L}(e^+ e^-)$ as discussed previously.
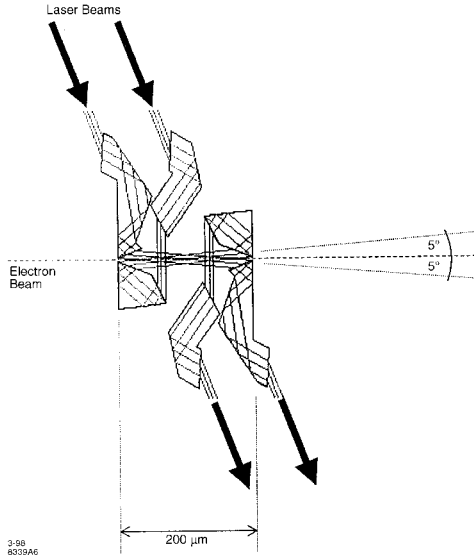
Fig. 3. A single, side-coupled laser cell to be fabricated in Silicon⟨100⟩.

Because these structures are to be fabricated in Si, they can be made deep enough to accommodate a true tensor structure with $n_y > 1$. This is shown in Fig. 4 for a single, thick wafer **or** a stack of such wafers using the same technology to provide accurate registration. Previously, we showed[5] that one can combine a vertical stack of bunchlets into a single, flat bunch with charge $n_y N_B$ with minimal radiative effects. Alternatively, we could simply accelerate flat beams using cylindrical lenses. This is clearly the simpler option to fabricate and provide beams for. Under the same assumptions as used above, one expects a luminosity $\mathcal{L} \approx 4n_y^2 \mathcal{L}(e^+ e^-)$. If we decrease N_B, we must then increase n_y to maintain the same total luminosity $\mathcal{L}$.
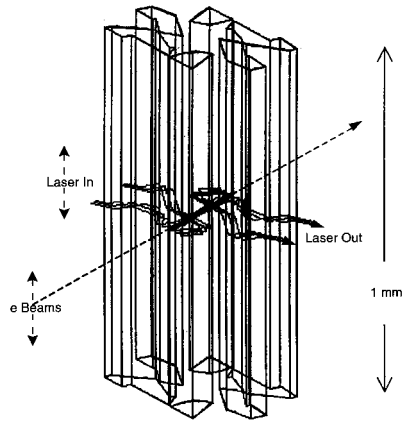

Fig. 4. 3D schematic of a single, side-coupled laser acceleration cell.

To maintain the overall phase coherence between cells, an electro-optical phase element can be included to control the phase and a group delay element to match individual cells to the electron(or positron) bunch in each cell. The spacing between linear arrays can contain active phase control elements such as one would need if they intended to use it for arbitrarily charged beam species. Although this suggests a very significant research development, the various technologies that are required are available now at reasonable costs and these are improving rapidly − at scales related to Moore's 'law'. This can not be said for the next generation RF structures either in terms of their fabrication technologies or their power sources because there is little, if any, commercial interest nor any apparent attempt to sponsor one.

A drive laser system such as required is suggested in Fig. 5. It could be used, in various forms, to drive a pin-cushion cathode to produce tensor beams or as a power source for the accelerator such as shown in Fig. 4 or previously[5] (see Fig. 5).
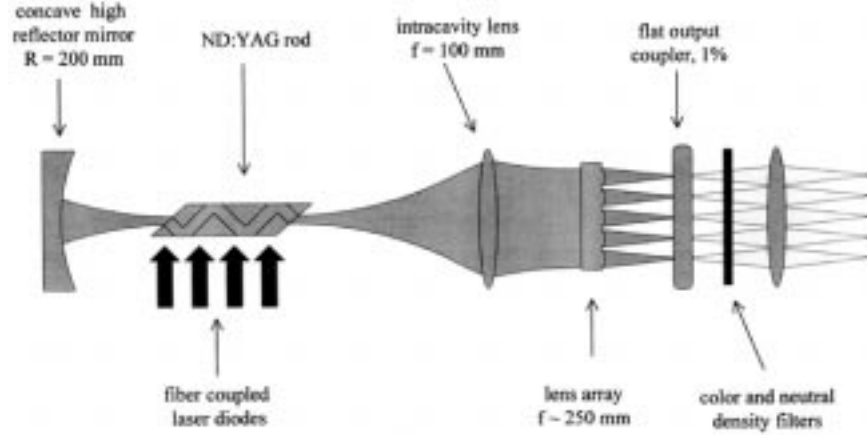

Fig. 5. Schematic of a multibunch laser driver for both source and accelerator.

4. Problems and Opportunities for Multibunch/Multibeam Operation

Such high frequency structures, whatever their specific form, are naturally suited to using smaller, lower emittance bunch charges − at least in one transverse direction. The Si technology advocated by Prof. R.L. Byer[15] implies a laser wavelength $\lambda \approx 2.5$ μm. For matched beams, this gives an invariant emittance for the particles

$$\epsilon_n = \tfrac{\lambda}{2} = 0.20 \ \mu\text{m} \implies N_B \leq 10^9 \ .$$

The undisrupted, rms spot size σ^* at a round focus is

$$\sigma^* = \left(\frac{\epsilon_n \beta^*}{\gamma_\beta}\right)^{\frac{1}{2}} = \frac{0.23}{\sqrt{\beta E(GeV)}} \ \mu\text{m} \quad \text{for} \quad \epsilon_n = 0.2 \ \mu\text{m}, \ \beta^* = 0.5 \ \text{mm} \ .$$

With these characteristics in a 'second generation' collider we expect

$$\mathcal{L}(ee) \approx 1.5 E(GeV) H_D \zeta \cdot 10^{32} \ \text{cm}^{-2}\text{s}^{-1} \quad \left(f_T = 10^4, n_x = n_y = n_q = 1, n_z = 100, N_B = 10^9 \right) \ .$$

For low D, $H_D \zeta \approx 1$ so that $\mathcal{L}(50 \ GeV) \approx 7.5 \cdot 10^{33}$ cm^{-2}s^{-1}. This is quite important for the experiments of interest. Assuming 10 kHz is available and 20% wall-plug efficiency, this implies 800 kW/m for an effective accelerating gradient of 1 GV/m.

$\mathcal{L}(ee)$ is proportional to incident energy if the other parameters are independent of energy as discussed[5] before. However, Richter discussed how typical non-resonant processes scale[16] as E^{-2}. No attempt was made to partition the charge N_B into smaller bunches or define the range of the tensor indices beyond giving a benchmark, average current of 160 μA for an integrated luminosity, over one Snowmass year, of 75 fb^{-1}. Clearly, even if the unused laser photons could be recycled, there would still be aperture radiation effects requiring a different distribution of the charge density. Another reason for Si, again related to its excellent thermal conductivity, is the possibility of embedding active, particle-beam control elements in it.

According to Byer, the diode drivers can be expected to reach $\approx 1\$/$W in this decade based on a Moore's law progression. The required laser is presumably not Nd:YAG as shown in Fig. 5 but Cr-doped ZnSe which presently doesn't exist in the desired form but possibilities such as discussed are now under serious study.

5. New Physics for a Low-Energy, High-Luminosity Prototype GLC

While e^+e^- has pinch enhancement, e^-e^- is cleaner than all of the other possible channels[17] because it is constrained by charge and lepton number conservation. With sufficient luminosity, this channel provides some unique opportunities[18,19] for physics at SLC energies. For $e^{\pm}e^{\pm}$, there is the possibility of dilepton gauge bosons having charges $Q=\pm 2$. At $\sqrt{s}_{ee}$= 100 GeV, the cross section in Frampton's 3-3-1 model[18] is $\approx$10 fb and there are essentially no background processes, e.g., the reaction e$^-\gamma{\rightarrow}Y^=e^+$ should be down by order α – remembering that $N_\gamma \leq 1$.

Another important reaction results when one converts one of the polarized e^- beams to $\vec{\gamma}$ for the reaction $\vec{e}_L\vec{\gamma}_R{\rightarrow}W\nu$ at comparable energies[3,19] of $\sqrt{s}_{ee}$= 120 GeV. Using 60 GeV electrons and frequency quadrupled Nd:YAG gives $\sqrt{s}_{e\gamma} \leq$ 110 GeV. In lowest order, the exchange diagram depends on a three gauge boson vertex. The three allowed coupling parameters allowed under CP are determined by the charge Q_W, the magnetic dipole moment μ_W and the electric quadrupole moment $\mathcal{Q}_W$. To see any deviations from point-like moments of the standard model, it is necessary to get sufficiently above the W-production threshold[20] to enhance both the magnitude *and* the sensitivity of the cross section to these effects.

Similarly, the $e\gamma{\rightarrow}eZ$ channel is interesting for the same reasons. Further, with $\vec{e}_R$ and high luminosity, one could also search for the lowest mass selectron $\tilde{e}$ and, finding it, study SUSY and try to determine its breaking parameters. There are other interesting possibilities but these reactions are important and are capable of testing every aspect of a GLC at SLC energies.

6. Comparisons to Actual Colliders

To be realistic, it is useful to consider some past results. For storage rings, the highest e^+e^- luminosity we are aware of is about 10^{33} at the B-Factories. For linear colliders, disruption enhancement has been observed at SLC[21] but at much lower $\mathcal{L}$. In this case, note that for $R=2.3$, $N_B=4{\cdot}10^{10}$ and $f_T=120$, one finds

$$H_+{\approx}H_x^{\frac{1}{2}}H_y^{\frac{1}{3}}=1.8 \implies \mathcal{L}_+(\text{SLC})=2.8{\cdot}10^{30} \quad \text{and} \quad \mathcal{L}_-(\text{SLC})=1.2{\cdot}10^{30} \quad \text{cm}^{-2}\text{s}^{-1}.$$

This gives a ratio $\mathcal{L}_+/\mathcal{L}_- =1.5$ comparable to what one found for Fig. 2 because the $f_b\#$, $f_l\#$ and R parameters, although intermediate, are closer to those values. Although the disruption is nonnegligible and the bunch length is reasonably short ($f_l\#\gtrsim2.5$), the enhancement is more due to f_l. Superficially, this suggests that SLC should have gone to flatter beams[22] and greater disruptions assuming this maintained acceptable backgrounds. Even so, the magnitude of $\mathcal{L}$ would never be enough for the experiments just discussed.

7. Concluding Discussion

We have tried to understand the important parameters and how they determine luminosity. Only three parameters are required to analytically represent results of large PIC simulations for $\mathcal{L}$ and only one[23] to constrain them for what is considered to be usable luminosity $\mathcal{L}_{\text{eff}}$. We called these parameters $f_b\#$, $f_l\#$, R and Υ_{eff}. We showed only two plots of the $e^\pm$ enhancement factor $H_\pm(f_b\#)$ for two values of $f_l\#$ corresponding to round ($R=1$) and flat beam ($R=63$) configurations with constraints on Δ_B, N_γ and Υ based on using Υ_{eff}. Corresponding plots for the constraint parameters were also generated but not shown because there were no serious discrepancies between the analytic prescriptions and the PIC simulations with the possible exception of Δ_B (≤ 20 %). This gets worse with increasing D because multiphoton emission is not included but this is not a problem for the regime of interest. Flat beams were understood to favor e^+e^- in order to allow larger D's i.e. smaller f_b-stops. The e^-e^- channel prefers this to be done with lower emittance rather than smaller f_l-stops.

However, from the perspective of every channel in a GLC, 'weak-focusing' is preferred. Even for γ channels, where one tries to use disruption to reduce the low energy $\mathcal{L}$, this leads to a serious disposal problem since D varies inversely with energy. Thus, 'disruption' is truly an apt description. Although it was verified[21] at the SLC, it appears highly overrated and isn't necessary even for e^+e^-.

Rather than large N_B and superdisruption, we proposed the opposite extreme of 'weak-focusing' with lower bunch charges but more bunches. This offers substantial improvements[5] in both power utilization and usable luminosity. Although this is imposed on us by the use of lasers, it allows much higher pulse rep-rates f_T and the very well developed fabrication technologies for silicon integrated circuits as well as the rapidly developing field of high-power, semiconductor laser diodes to replace klystrons. It also implies lower invariant bunch emittances that appear easier and cheaper to obtain but this requires qualification and will be discussed elsewhere.

Several bunch combination/distribution schemes were discussed. For example, combining bunches vertically or accelerating flat bunches allows higher D and also enhances $\mathcal{L}$ quadratically with n_y without requiring damping rings. Bunches can also be combined horizontally that gives a combined bunch that is much shorter than the producing train. In this regard, all channels benefit if charge compensation is implemented because this provides the added advantage that it would increase luminosity and reduce backgrounds. Regardless, combining short bunches provides

an additional option for bunch shaping beyond the conventional use of chicanes and RF for longitudinal optics. Although none of the above violates anything fundamental (Liouville, exclusion principle, radiative broadening, Cauchy-Riemann constraints) this subject clearly requires further discussion and demonstration.

The question of scalability[5] with λ is a problem for both λ_{RF} and λ_{laser} where one wants to decrease λ_{RF} and increase λ_{laser}. It has been shown[5] that shorter wavelengths imply larger n_x, n_y, n_z and f_T as well as bunch combination. This leads to what may be called capillary (CW) beams that provide unforeseen benefits beyond the common problems of wake effects, power dissipation and the coupling of microwave or infrared power into structures and then into the particle beam.

While we have argued the advantages of Moore's 'law', it is only useful when accompanied with enhanced source and detector bandwidth. The paradigm called Amdahl's 'law' required memory and I/O bandwidth to scale with the processor improvements for optimal system utilization. This implies that the detector must be capable of one event per bunch crossing which implies faster, larger buffers. Likewise, the 'pin-cushion' source, based on true field emission, should provide high rep-rate, stable operation for which there is considerable commercial justification.

The SLC was a prototype that did Z physics and verified a number of machine physics effects. A prototype GLC appears practical on the same basis. Further, we indicated how the proposed changes could provide an exponential growth in energy for linear colliders in the same way that has been enjoyed in the past for both[24] proton and electron storage rings. This was done by using a common, more fundamental measure rather than the conventional 'Livingston' plot. Exponential growth would end when a limit is reached that is fundamental to the process such as radiative losses in storage rings. While this will occur in linear colliders as well, it should not be built in through the use of fabrication techniques that are too expensive or that don't scale with energy in a realistic way.

8. Acknowledgements

References

1. **e-e-** 1995: Proceedings of the Electron-Electron Linear Collider Workshop, Ed. C.A. Heusch, Santa Cruz, CA, Sept. 4-5, 1995. *Intl. J. Mod. Phys.* **A11** (1996) 1523.
2. J.E. Spencer, Beam-Beam Effects and Generalized Luminosity, *Intl. J. Mod. Phys.* **11** (1996) 1675. See also SLAC-PUB-7051, January 1996.
3. J.E. Spencer, Uses of a Prototype NLC/GLC, *Nucl. Inst. Meth.* **A355** (1995) 1.

4. Zeroth-Order Design Report for the Next Linear Collider, May 1996, SLAC Report 474, LBNL-PUB-5424, UCRL-ID-124161.

5. J.E. Spencer, Limitations Imposed by Beam-Beam Effects and Their Remedies, *Intl. J. Mod. Phys.* **11** (1998) 2479.

6. K.L. Brown and J.E. Spencer, Non-Linear Optics for the Final Focus of the Single-Pass Collider, *IEEE Trans. Nucl. Sci.* , **NS-28** (1981) 2568.

7. Robert Hollebeek, Disruption Limits for Linear Colliders, *Nucl. Inst. Meth.* **184** (1981) 333.

8. A.W. Chao, Beam-Beam Instability, in *Physics of High Energy Particle Accelerators*, AIP Conf. Proc. No. 127 (1985) 202.

9. J. Spencer, J. Irwin, D. Walz and M. Woods, The SLAC NLC Extraction and Diagnostic Line, IEEE95CH35843, Proc's: 16th IEEE Part. Accel. Conf. and Intl. Conf. on High Energy Accel's., R. Siemann, Ed., Dallas, TX, (1995) 671.

10. K. Yokoya and P. Chen, Beam-Beam Phenomena in Linear Colliders, Proc's. Topical Course on Part. Accel's., LNP 400, Nov. 7-14 (1990) 415.

11. I use the designation δ_B consistently in Ref's. 2,4,5 based on conventional beam physics. Others use it for $\langle E_i - E_o \rangle / E_i$ which is called Δ_B here. In a related vein, I use the term 'beamsstrahlung' because it requires the presence of two beams.

12. P. Chen, Differential Luminosity Under Multiphoton Beamstrahlung, *Phys. Rev.* D**46** (1992) 1186.

13. K. Yokoya, ABEL, A Computer Code for the Beam-Beam Interaction in Linear Colliders, *Nucl. Inst. Meth.* **B251** (1986) 1 as well as T. Tauchi et al. *Part. Accel.* **41** (1993) 29.

14. D. Schulte, Guinea Pig: A Beam-Beam Interaction Simulation Program, Available under UNIX at http://www-sldnt.slac.stanford.edu/nlc/programs/. I would like to thank Kathy Thompson for her help with learning to use this setup.

15. T. Plettner, R.L. Byer and Y.C. Huang, (Ginzton Labs); R.L. Swent and T.I. Smith (HEPL); C. Barnes, E. Colby, R.H. Siemann, J.E. Spencer and H. Wiedemann (SLAC), The Laser Electron Acceleration Project (LEAP).

16. B. Richter, Very High Energy Electron-Positron Colliding Beams for the Study of Weak Interactions, Workshop on Gamma-Gamma Colliders, *Nucl. Inst. Meth.* **136** (1976) 47.

17. Clemens A. Heusch, $e^- e^-$ Physics at an $e^- e^-$ Collider, Workshop on Gamma-Gamma Colliders, *Nucl. Inst. Meth.* **A355** (1995) 75; also *Intl. J. Mod. Phys.* **11** (1996) 1523.

18. P.H. Frampton, Chiral Dilepton Model and the Flavor Question, *Phys. Rev. Lett.* **69** (1992) 2889 as well as this Workshop.

19. J.E. Spencer, The SLC as a Second Generation Linear Collider, IEEE95CH35843, Proc's: 16th IEEE Part. Accel. Conf. and Intl. Conf. on High Energy Accel's., R. Siemann, Ed., Dallas, TX, (1995) 671.

20. LEP-II determines mass M_W much better than this reaction but not these quantities.

21. T. Barklow, G. Bower, F.J. Decker, C. Field, L.J. Hendrickson, T. Markiewicz, D.J. McCormick, M. Minty, N. Phinney, P. Raimondi, K.A. Thompson, T. Usher, M.D. Woodley, F. Zimmerman, Experimental Evidence for Beam-Beam Disruption at the SLC, Proc's: 17th IEEE Part. Accel. Conf., New York, NY, (1999) 307.

22. P. Raimondi, M. Breidenbach, J.E. Clendenin, F.J. Decker, M. Minty, N. Phinney, K. Skarpass VIII, T. Usher, M.D. Woodley, Luminosity Upgrades fo the SLC, Proc's: 17th IEEE Part. Accel. Conf., New York, NY, (1999) 3384.

23. For a GLC, we would have to include another, external, strong field parameter $\Upsilon_{\text{eff}}^{\text{ext}}$.

24. J.E. Spencer, Optimal, Real-Time Control – Colliders, Proc's: 1991 Part. Accel. Conf., San Fran., CA, (1991) 1440.